

Effect of pomegranate peel extract on shelf life of strawberries: computational chemistry approaches to assess antifungal mechanisms involved

D. Rongai¹  · N. Sabatini² · P. Pulcini¹ · C. Di Marco² · L. Storchi^{3,4} · A. Marrone³

Revised: 11 April 2018 / Accepted: 23 April 2018 / Published online: 30 April 2018
© Association of Food Scientists & Technologists (India) 2018

Abstract In Italy *Botrytis cinerea* represents the most significant disease in strawberry crops and causes major quality and quantity losses in postharvest storage. An alternative strategy to the synthetic fungicides in crop defence could be the use of bioactive compounds with high antifungal activity. This research regards the use of *Punica granatum* peel extract to extend the shelf life of strawberry and the proposal of a possible mechanism for its antifungal activity. In vitro and in vivo tests showed the ability of pomegranate peel extract to control strawberry gray mould. Fourier transform near infrared spectroscopy showed a high correlation between spectra and disease severity then, a putative molecular mechanism for the interaction of punicalagin on ergosterol of fungal membrane was described by means of computational chemistry approaches. Molecular dynamics simulations were performed by using Gromacs to gain multiconformational representations of either punicalagin and an antifungal compound of clinical relevance, i.e. amphotericin B. The use of grid-based procedures, allowed to shed some light on the molecular mechanism featuring the antifungal activity of punicalagin.

Keywords Gray mould · Punicalagin · Postharvest diseases · Ergosterol · Computational chemistry

Introduction

Botrytis cinerea, also known as gray mould fungus, causes serious postharvest diseases in many plant species including strawberry (*Fragaria x ananassa* Duch.). It stands in the world's top 10 fungal plant pathogens of economic importance. The fungus infects various parts of the strawberry plant, such as leaves, flowers and fruits, in different ways, but the main cause for the decline of mature fruit after harvest occurs when the fruits are infected in the very early stages of development through senescent flowers. Italy is one of the most important producers of strawberries and *B. cinerea* represents the most significant disease which causes major quality and quantity losses in postharvest storage. In order to extend the shelf life, strawberries are harvested and placed in a cold box and/or harvested in the early morning. In fact, strawberry shelf life is 1 day shorter when harvested after 10 AM (Romanazzi et al. 2016). To control the fungus spread into the crop, synthetic fungicides are normally applied by treatments during flowering in order to reduce fruit infection. Nevertheless, the large use of synthetic fungicides in crop defence leads to resistance problems and serious risks to the environment and human health. An alternative strategy could be biological control, using antagonist micro-organisms with high antifungal activity. For instance, the yeast *Cryptococcus albidus* sprayed all through the bloom of strawberry reduced the postharvest incidence of disease on fruits by 33, 28 and 21% in 1997, 1999 and 2000, respectively (Helbig 2002). More recently, several authors have investigated the antifungal activity of a large number

Electronic supplementary material The online version of this article (<https://doi.org/10.1007/s13197-018-3192-0>) contains supplementary material, which is available to authorized users.

✉ D. Rongai
domenico.rongai@crea.gov.it

¹ CREA Research Centre for Plant Protection and Certification, via C.G Bertero, 22, 00156 Rome, Italy

² CREA Research Centre for Engineering and Agro-Food Processing, via L. Petrucci 75, 65013 Città Sant' Angelo, Italy

³ (UNI-CH) Università degli Studi G. D'Annunzio Chieti-Pescara, via Vestini 31, 66100 Chieti, Italy

⁴ Molecular Discovery Limited, Middlesex, London, UK

of more environmentally friendly natural formulations, that could be suitably applied in place of fungicides in the treatment of strawberry. Some of these contain glutathione, oligosaccharides, laminarin and chitosan, substances able to inhibit postharvest decay because of their dual action: (1) direct inhibition of fungus, and (2) stimulation of the natural defence mechanisms (Landi et al. 2014). Many natural compounds either vegetable-derived, such as alliin, glucosinolates, essential oil from oregano, savory and thyme, or animal-derived compounds, have been reported to be effective against gray mould infection (Lopez-Reyes et al. 2010; Nabigol and Morshedi 2011). Other alternative strategies such as disinfecting agents (used for fruit surface sterilization in postharvest packaging) or physical treatments (UV-C irradiation, ozone hypobaric and hyperbaric applications) have also been studied (Mlikota Gablera et al. 2010; Romanazzi et al. 2012). However, the control of *B. cinerea* by preharvest strategies is only partially successful may be because the fungus has several ways of infecting strawberry plants. The control of gray mould infection in the postharvest stage is expectedly more feasible during storage (Romanazzi et al. 2013). The aim of the present study was to investigate the *in vitro* and *in vivo* activity of pomegranate peel aqueous extract on *B. cinerea* in strawberry. *Punica granatum*, commonly known as pomegranate, is an important source of bioactive compounds (Rongai et al. 2015). The antimicrobial activity of pomegranate peel extract is linked to a high level of phenolic and flavonoid content (Rongai et al. 2017). The presence of the main antifungal compounds (punicalagins and ellagic acid) in the extract is also determined through a simplified HPLC–MS–MS analytical method (Fischer et al. 2011). The possible mechanisms involved in the antimicrobial activity of the punicalagins were also investigated by means of computational chemistry. Fourier transform near infrared (FT-NIR) spectroscopy is considered a non-destructive, potent instrumental method for food quality control of a large number of products such as milk, butter, cheese, meat, fruit, and more recently for olive fruits and virgin olive oil (Bendini et al. 2007). Spectral measurements were taken on strawberry fruits in reflectance mode using an FT-NIR spectrometer (PERKIN ELMER). The main purpose of this research was to evaluate the potential application of the pomegranate peel extract to maintain fruit quality and extension of strawberry shelf life. Moreover, the identification of punicalagin as the major component of the pomegranate peel extract made it possible to propose hypotheses on the possible mechanism of its antifungal activity. Thus, the molecular properties of punicalagin were also investigated and compared with those of amphotericin B, one of the first choice antifungal molecules, by the use of computational approaches.

Materials and methods

Fruits and fungus used

Strawberry (*Fragaria x ananassa* Duch.) fruits were obtained from a commercial market of organic products. The fruits of uniform size, no defects and the same degree of ripening were selected.

B. cinerea (strain CREA-DC Roma collection number 1623) was maintained on potato dextrose agar (PDA, OXOID CM 0139) and stored at 4 °C. When needed, the isolate was grown for 8 days on PDA in the dark at 25 ± 2 °C.

Pomegranate peel extract used

Samples of *P. granatum*, var. dente di cavallo, provided by the botanical garden at “CRA-DC”, Rome, Italy, were used. The powder of extract was obtained according to the method described in (Rongai et al. 2017). Pomegranate peel were cut into small pieces and added to solvent; this was 100% of water or 50% of water (bidistilled water from a Milli-Q-System, Millipore, Bedford, UK) mixed with 50% of ethanol (analytical grade RPE, Carlo Erba Reagents, Milan, Italy). The mixture was agitated overnight at 40 °C, before sonicating for 15 min. The ethanol was evaporated and the extract obtained was centrifuged and the supernatant filtered through 0.45 µm PTFE filter. The obtained pomegranate peel aqueous extract (PAE) and pomegranate peel aqueous + ethanol extract (PAEE) were stored in a freezer at – 20 °C until further use. For all treatments only PAE was used.

Chemical analysis HPLC–MS–MS–ES(–)

PAE and PAEE were analyzed according to the method described in (Rongai et al. 2017). Samples were reconstituted with methanol to obtain a 0.5 mg/mL concentration, filtered on PTFE 0.45 µ, then a 20 µL volume was injected in the Micromass 4micro triple quadrupole system (Waters), equipped with a Waters Alliance 2695 separation module and 2695 Alliance autosampler, Waters 2487 Dual λ Absorbance Detector, Waters 4micro MSD (mass spectrometry detector) with Electrospray Ionisation (ESI) interface, connected in series.

HPLC separation was carried out with a RP C18 analytical column (Phenomenex, Kinetex EVO 5 µ, 100 Å, 150 × 46 mm) operating at 30 °C. The dual wavelength detector performed simultaneous monitoring at 280 and 320 nm. The mobile phase consisted of acetic acid in water 2% (v/v) (eluent A) and acetic acid in methanol 2% (v/v) (eluent B). The flow rate was constant at 0.9 mL min^{–1}

split for the MSD with a split ratio of 7:3. Data acquisition and processing were performed with MassLynx 4.1 software. The ESI interface operated in Negative (ES⁻) and with the MRM (multiple reaction monitoring) mode, monitoring two *m/z* mass transactions for each component investigated.

Fourier Transform Near Infrared (FT-NIR) spectroscopy

Spectral measurements were taken on strawberry external surface in reflectance mode using an FT-NIR spectrometer (PERKIN ELMER). Sixty-four scans were performed for reflectance spectrum in about 30.1 s, range 10.000–4.000 cm^{-1} , spectrum resolution 16 cm^{-1} . The chemometric model was constructed with the PCR/PLS software implemented in the Perkin Elmer spectrometer by setting the full cross validation type (leave one out), and four PCs. A preliminary search of a chemometric NIR model on strawberry fruits to predict disease severity was carried out. The model building was performed by means of multi linear regression of principal components (PCR) of the matrix made up of the spectra (independent variables) versus the numerical value of disease severity (dependent variable).

Computational chemistry

Molecular dynamics simulations of Amphotericin B (AmB) and punicalagin (p-alagin) were performed by using Gromacs (Van Der Spoel et al. 2005). Each molecule was placed in a cubic box preventing self-interaction, and solvated with water molecules. Each system was optimized and slowly heated up before production run of 500 ns at 300 K in NPT ensemble, using the velocity rescaling scheme (temperature) and the isotropic Berendsen coupling scheme (pressure) (Berendsen et al. 1984). All molecular systems were simulated in the Gromos 54a7 force field, with the LINCS constrain algorithm (Hess et al. 1997), and electrostatics computed by the Particle Mesh Ewald method (Darden et al. 1993). Numerical trajectory analyses were carried out by the use of either Gromacs utilities. Ensembles of 5000 conformations per trajectory were extracted and clusterized on heavy atoms by using the *g_cluster* utility (Daura et al. 1999). The middle structures of the clusters (coverage > 80%) formed two subsets representing AmB and p-alagin in an aqueous bulk. Each representative conformation was optimized in the OPLS-2005 force field (Kaminski et al. 2001) and using the GB/SA polarisable continuum solvation method (Di Qiu et al. 1997) with the MacroModel software (version 9.8, Schrödinger, LLC, New York, NY, 2010).

The GRID program was used to calculate the molecular interaction field (MIF) of O (*sp*² carbonyl oxygen), N1 (Neutral flat NH e.g. amide) and OH₂ (water) probe for each AmB or p-alagin configuration (Cross and Cruciani 2010). MD weights were used to calculate final weighted average MIFs. All MIF computations were performed using a parallel version of the code based on POSIX thread [Butenhof DR, Programming with POSIX threads, Addison-Wesley Longman Publishing Co., Inc. Boston, MA, USA (1997)] as detailed elsewhere (Storchi et al. 2015). All software needed for MIF analyses was developed in Python language [Python tutorial, Technical Report CS-R9526, Centrum voor Wiskunde en Informatica (CWI), Amsterdam. www.python.org.] by use of modules NumPy (Jones et al. 2001) and Pybel (O'Boyle et al. 2008). All molecular graphics artworks were obtained by the use of Visual Molecular Dynamics (VMD) or Maestro (version 9.4, Schrödinger, LLC, New York, NY, 2013) software.

In vitro tests

Mycelial inhibition was assessed by measuring radial growth on 90 mm Petri dishes containing 20 mL of Potato Dextrose Agar (PDA). In treated plates, a total of 15, 30, or 60 mg of PAE was added to PDA as the media was about to gel (50 ± 3 °C) such that the concentration corresponded to 0.75, 1.5, or 3% (w/v), respectively. In untreated plates (negative control), samples contained PDA without extract. A plate containing a standard fungicide (Marisan 50 PB, Dichloran 60%, SIAPA, Milan, Italy) was used at the recommended concentration as a positive control. A 5 mm diameter plug of inoculum was taken from the actively growing margin of 6–10 day-old cultures of *B. cinerea* and aseptically placed face up in the centre of each Petri plate. There were four replicates per treatment and the test was repeated twice. Plates were incubated at 24 ± 2 °C, radial growth was measured each day, starting 3 days after inoculation, until the plates were overgrown. Inhibition by each extract was calculated by the formula: % inhibition = $100 \times (\text{colony diameter (mm) of control} - \text{colony diameter (mm) of sample}) / \text{colony diameter (mm) of control}$.

Each treatment was replicated four times and the test was repeated twice.

In vivo tests

Selected strawberries were immersed for 30 s in a 2 L volume of the respective solutions. Fruits soaked in deionized water were used as the control. The fruits were then dried in air for 1 h and arranged in groups of 18 in plastic boxes containing three absorbent layers on the bottom. After treatments, strawberries were stored for

2 days at 0 ± 1 °C, 95–98% of relative humidity, and then at 20 ± 1 °C, 95–98% of relative humidity for another 3 days (shelf life).

Each treatment consisted of 72 fruits (18 fruits \times 4 replicates) and included: (a) non treated control; (b) fruits treated with PAE at the concentration of 0.75%; (c) fruits treated with PAE at the concentration of 1.5%; (d) fruits treated with PAE at the concentration of 3%.

Disease severity (DS), disease incidence (DI) and Fourier transform near-infrared (FT-NIR) spectra were recorded. An empirical scale was designed for this experiment. DS was recorded on a 0–5 scale where: 0 = no symptoms; 1 = 1–20% fruit surface infected; 2 = 21–40% fruit surface infected; 3 = 41–60% fruit surface infected; 4 = 61–80% fruit surface infected; 5 = more than 81% of the strawberry surface infected and with sporulation. The percentage disease severity of each treatment was calculated by the formula: $DS \% = (\text{sum of all disease ratings} \times 100) / (\text{total number of ratings} \times \text{maximum disease grade})$. Disease incidence was determined according to the formula: $DI \% = (\text{No. of infected plants} \times 100) / (\text{Total no. of plants assessed})$.

After the NIR test, strawberry fruits belonging to the highest dose treatment (3%) and the untreated control were homogenized and stored for 1 week at 4 ± 1 °C and 50–60% of relative humidity. Antifungal activity of PAE was also evaluated through direct observation of homogenized samples. The test was repeated three times.

Statistical analysis

Mycelial growth inhibition, disease severity, and disease incidence were analysed by ANOVA with means separation by Fisher's protected LSD test at $\alpha = 0.05$. Because the results from two independent experiments were consistent and there were no interactions between experiment run and treatments, data from two independent experiments were combined and the experiment was treated as a block term in the analysis. To correct for heterogeneity of variance, the data were arcsine-transformed prior to analysis. SigmaPlot V10 (London, UK) was used to create graphics and Sigma Stat V3.5 (London, UK) was used for ANOVA.

Results and discussion

Chemical analyses of *P. granatum* peel extract

The PAE and PAEE were analyzed with HPLC–MS–MS to identify punicalagins, the main components of *P. granatum* peel. In Fig. 1, the mass spectrometry (MRM) chromatograms and relative m/z ion fragments confirm the identity of punicalagins, and show that the area of peaks is

slightly more extended in the aqueous extract (B) than the hydro-alcoholic extract (A). These data are essentially in agreement with previous evidence (Rongai et al. 2017). The authors claimed that the larger the area of chromatogram peaks, the greater the antifungal activity and that, although there were no significant differences between PAE and PAEE, the first was slightly more effective. The findings were also in agreement with Foss et al. (2014) who sustained that the isolated compound of punicalagin showed the same antifungal activity as the crude extract. The lack of difference between extract and pure substance is probably due to the fact that the punicalagin is, as noted above, the main substance in the pomegranate fruit peel.

In vitro tests

In vitro antifungal activity of PAE against *B. cinerea* was demonstrated by detecting that, 3 days after inoculum, the mycelia growth was 53.7 mm in the control plates while it significantly decreased to 32.7 (0.75% of concentration) or 18.0 mm (3%) in plates with extracts. Six days after inoculum, the control plates were entirely invaded by the fungus while in plates with extracts the mycelia growth peaked at values between 41.7 (0.75% of concentration) and 31 mm (3%). There were no significant differences in mycelial growth at the fifth day among concentrations 1.5 and 3% (Table 1). This could be due to the fact that at higher concentrations the extract does not dissolve completely in the PDA, probably because the acidity is too high. However, at the sixth day, although there was not a great difference the 35.7 value recorded at the concentration of 1.5% was statistically higher than 31.0 recorded at the concentration of 3%. The above reported values of growth are consistent with a good antifungal activity of the PAE against *B. cinerea*, although a higher antifungal response of this extract with respect to *F. oxysporum* was already reported by Rongai et al. (2017).

In vivo tests

The ability of PAE to control gray mould of strawberry caused by *B. cinerea* was shown also at the lowest dose (Fig. 2). By increasing the concentration of the extract, both disease severity (DS) and disease incidence (DI) decreased: for the treatment with 0.75% extract we detected DS and DI at 29.33 and 66.6%, respectively, both values are considerably lower than 74.66 and 93.33% obtained in the untreated control. No statistically significant difference was detected at concentrations between 0.75 and 1.5%, whereas at 3% the extract was seemingly more effective, e.g. with values of DS and DI of 19.3 and 40%, respectively (Fig. 3). Hence, PAE reduced the disease severity and incidence of gray mould.

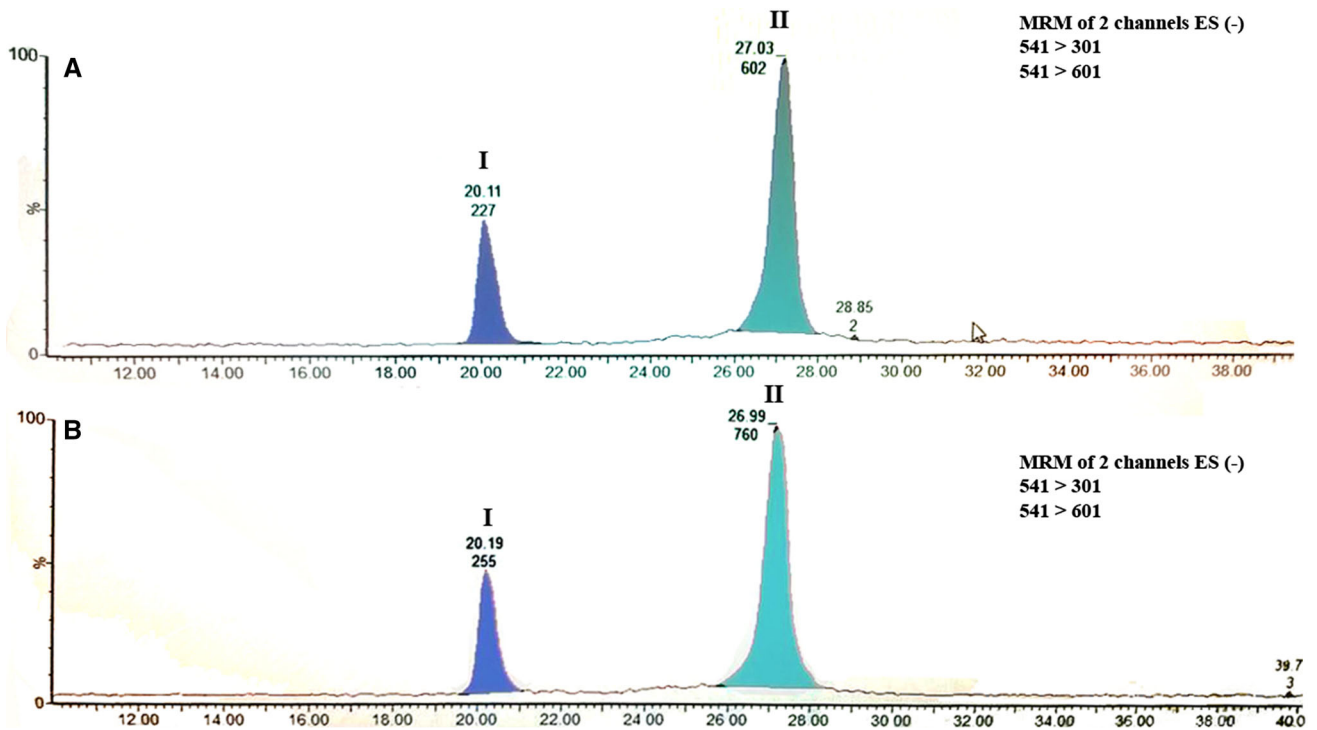


Fig. 1 HPLC-MRM mass spectrometry chromatograms and relative m/z ion fragments of punicalagins I and II of *P. granatum* hydro alcoholic peel extract (a) and *P. granatum* aqueous peel extract (b)

Table 1 In vitro inhibition of mycelial growth of *B. cinerea* by increasing doses of pomegranate peel aqueous extract (PAE)

Treatment	Mycelia growth of <i>B. cinerea</i>			
	3th day mm	4th day mm	5th day mm	6th day mm
Untreated control	53.7 ± 0.33a	60.2 ± 0.09a	69.0 ± 0.33a	89.5 ± 0.10a
PAE (0.75%)	32.7 ± 0.27b	34.0 ± 0.18b	37.5 ± 0.33b	41.7 ± 0.23b
PAE (1.50%)	26.0 ± 0.29c	28.3 ± 0.08c	29.5 ± 0.12c	35.7 ± 0.17c
PAE (3%)	18.0 ± 0.14d	21.0 ± 0.08d	28.8 ± 0.17c	31.0 ± 0.11d
	F = 128.74	F = 833.34	F = 216.18	F = 1078.83
	P < 0.001	P < 0.001	P < 0.001	P < 0.001

Values with different letters for each group are statistically different (LSD test, $\alpha = 0.05$). Standard deviations of the means are indicated

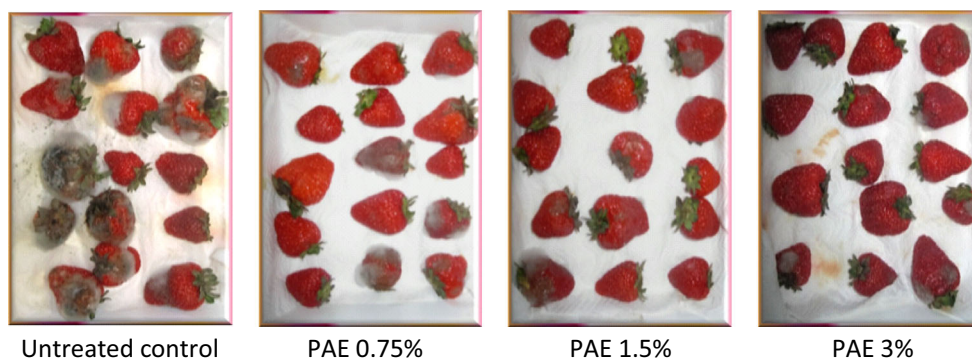


Fig. 2 Effects of the extract (0.75, 1.5 and 3% w/v) on strawberry fruits 7 days after treatments

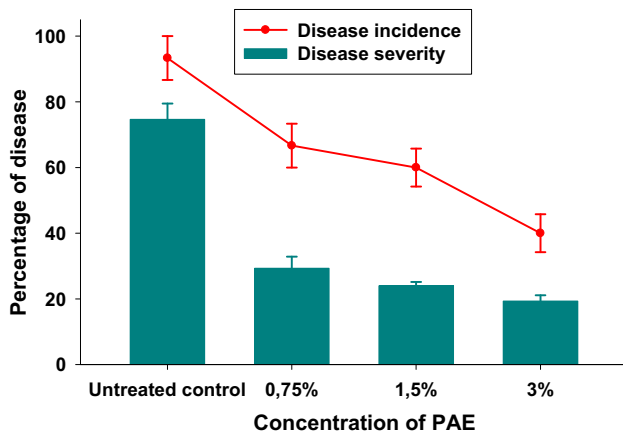


Fig. 3 Pomegranate aqueous peel extract (PAE) effect on disease incidence (DI) and disease severity (DS) on *Botrytis cinerea*

FT-NIR spectroscopy

FT-NIR performed on strawberry surface showed a high correlation between spectra and disease severity used as analytical property. In fact, The NIR data showed a significantly different spectrum between the untreated control and treated fruits. The effectiveness of PAE was also confirmed by the chemometric predictive model built through the employment of DS and NIR spectra. Principal component regression analysis (full cross validation type) showed a percentage of variance (R^2) = 98.8% and F value = 99.5. Standard error of prediction (SEP) and of estimation (SEE) were 5.685 and 3.048, respectively.

In Figure S1 (supplementary material), stretching and vibrational second overtone for the CH bond in $-\text{CH}_3$, $-\text{CH}_2$, and $-\text{HC}=\text{CH}-$ groups ranged in the interval $7800\text{--}9000\text{ cm}^{-1}$. OH stretching of first overtone ranged between 6000 and 7800 cm^{-1} , while the peak in the $4500\text{--}5500$ interval is ascribed to water. Finally, the short peak detected between 4000 and 4400 is a combination of $-\text{CH}$ stretching vibrations of CH_3 and CH_2 groups.

Furthermore, the antifungal activity is also confirmed by direct observation of the homogenized strawberry fruits. The samples treated with the highest dose were seemingly fungal free if compared with the corresponding untreated controls. In fact, untreated homogenized samples were completely invaded by gray mould, while those treated with PAE appeared clearer and healthy (Figure S2-supplementary material).

Acidic properties of phenol

The antifungal activity could be due to the interaction between extract compounds (punicalagin) and fungal membrane structure (Figure S3-supplementary material).

The effects of PAE on fungi cell membrane are linked to the biochemical phenolic properties. These compounds are weak organic acids ($\text{pK}_a \sim 4.2$) and are known to have membrane-active properties against microorganisms causing leakage of cell constituents including proteins, nucleic acids, and inorganic ions such as potassium or phosphate (Johnson 2003). Phenols may diffuse through the cytoplasmic membrane by passive diffusion (Fick law) in their undissociated form, increasing its permeability, altering cell membrane structure and causing protein denaturation. Some authors found that lowering pH by adding phenols in wine could facilitate the diffusion of phenolic acids through the cytoplasmic membrane and that other antimicrobial agents may have synergistic effects with these compounds on the bacterial membrane. Furthermore, some authors showed that phenolic compounds exert an antifungal activity by hindering the synthesis of ergosterol, glucan, chitin, proteins and glucosamine. Ergosterol, a sterol from the lipid class, is an important component of fungal cell membranes. The high water solubility and acidity of phenols and polyphenols like punicalagin is also explained by delocalization by means resonance of the negative oxygen charge of the ionized form in ortho and in para of the aromatic-benzene ring. Phenols have an $-\text{OH}$ group directly linked to a benzene ring. When the hydrogen-oxygen bond breaks, a phenoxide ion, $\text{C}_6\text{H}_5\text{O}^-$, is generated.

When the pH value is less than the phenol's pK_a ($-\log K_a$), the undissociated form predominates, and can pass through the organic phase of the double phospholipid layer of the fungi cellular membrane. If the pK_a value is greater than the pH value, the ionized form, which is not similar to the organic phase, prevails.

When $\text{pH} = \text{pK}_a$, the concentrations of ionized and undissociated forms are equivalent. The undissociated form of phenols have the highest inhibitory effect of the fungi in vitro growth, probably due to the change of the membrane functionality and integrity, possibly by forming complexes with sugars, proteins and beta-ergosterol of fungi cellular membrane. Thus, the deficiency of beta-ergosterol may prejudice the cell membrane development and maintenance of its selective permeability. The interaction of punicalagin with ergosterol as well as for AmB (antifungal macrolide) may alter the fungal membrane functionality and integrity by the formation of aggregates acting as pores with a consequent loss of potassium, magnesium, sugars, and other metabolites necessary for survival of cells. Based on the assumption that punicalagin and AmB may similarly form pore-like aggregates responsible for their antifungal activity, the molecular interaction properties of both molecules were also investigated and compared through computational approaches.

Computational chemistry

AmB is a polyene macrolide antibiotic that has been employed for many years in the treatment of systemic fungal infections and is still the drug of choice in the antimicrobial therapy of severe infections (Ghannoum and Rice 1999). Although the molecular mechanism of action has not been completely clarified, it is reputed that AmB may disrupt the cell membrane functions through the formation of ion channels that alter the physiological transmembrane gradients and, eventually, lead to cell death (Hartsel and Bolard 1996). Consistently with the mostly accredited “sterol hypothesis”, sterol molecules are important to promote the formation of AmB aggregates in cell membranes: ergosterol—a component of fungal membrane—was found to be more effective than cholesterol—a component of animal membrane—in stabilizing the intramembrane aggregates of AmB, by the formation of mixed AmB-ergosterol supramolecular structures. Moreover, recent studies showed that the channel-forming capacity of AmB is not required for antifungal activity: by the use of nuclear magnetic resonance techniques it was detected that AmB forms extra-membrane rather than intramembrane aggregates that likely cause fungal death by extracting ergosterol from lipid bilayers (Anderson et al. 2014). Therefore, even in the absence of channel-like activity, the capability of these AmB aggregates to bind ergosterol is alone sufficient for antifungal activity. The AmB-sterol aggregates hypothesized by Baginski et al. (2002) are featured by a specific orientation of the AmB units with respect to the phospholipid leaflet. The inner wall of the hosting channel is formed by polyhydroxyl chains, whereas the unsaturated chains mainly interact with the apolar chains of the membrane lipids. On the other hand, the AmB zwitterionic groups formed the inlet edge of the channel and interact via polar contacts with the polar heads of the membrane lipids. The spatial arrangement of AmB units in the membrane aggregates is thus intimately connected to the “molecular anatomy” so that we can hypothesize that similar aggregates may be formed by some other molecule that resembles the AmB anatomy although belonging to a different class of compounds. By such an assumption, we considered whether the antifungal activity of p-alagin may be connected to its similarity with AmB and to the formation of analogous extra-membrane aggregates. The molecular similarity between AmB and p-alagin was investigated by the use of a previously reported computational workflow based on the combination of molecular dynamics (MD) simulation and grid-based molecular interaction field (MIF) analysis (Storchi et al. 2015; Marrone et al. 2016). MD made it possible to characterize the most representative conformations of AmB and p-alagin to gain a multiconformational (dynamic) picture

of the molecular structures. The calculation of MIF made it possible to feature the space surrounding each molecule with spots of high interaction, so that the structures of AmB and p-alagin may be compared in terms of their interaction similarity. The mapping of donor and acceptor hydrogen bond fields around AmB and p-alagin was obtained by the use of O and N1 probes, and led to the three-dimensional sketches reported in Fig. 4.

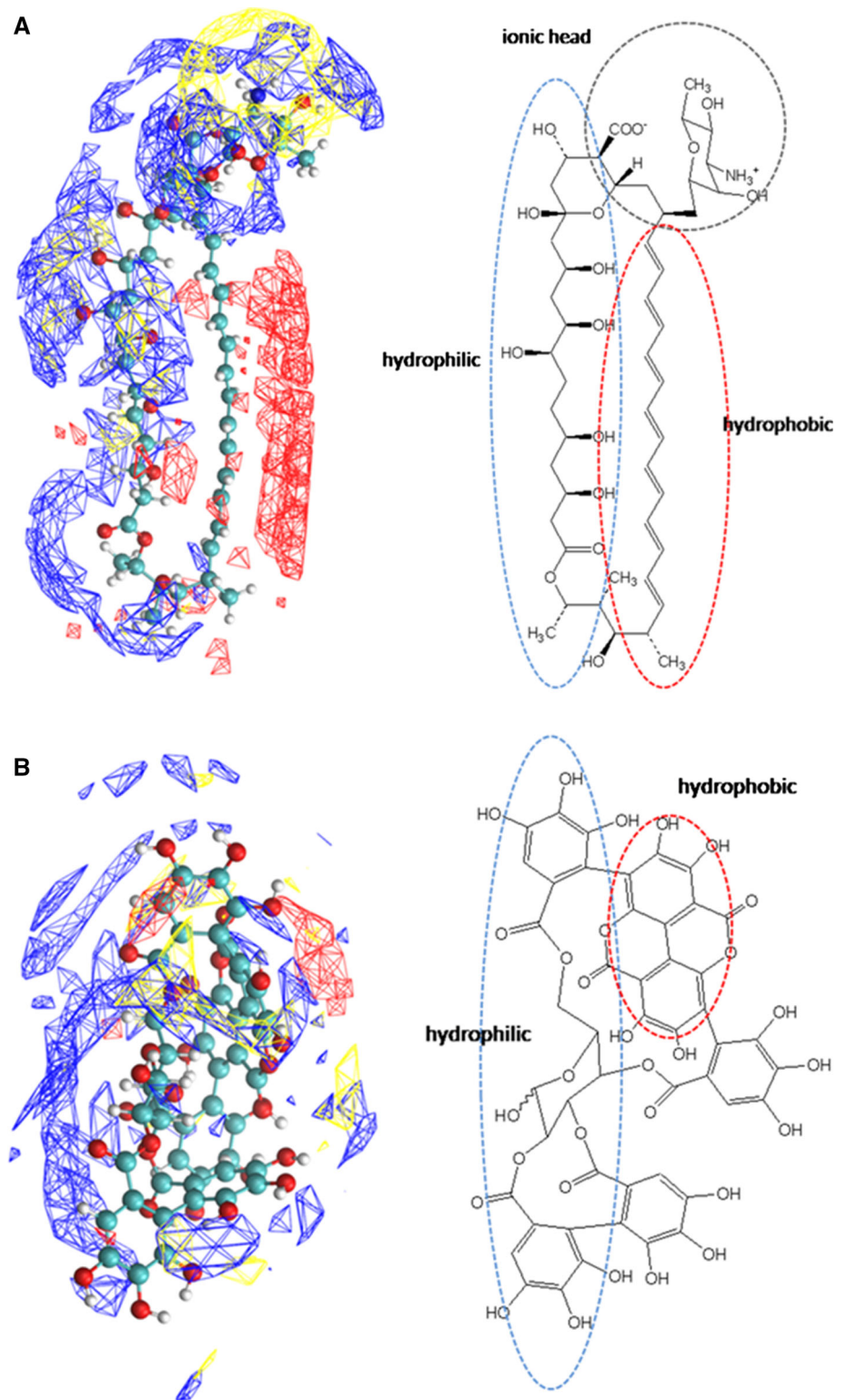
The polyhydroxyl chain of AmB is surrounded by a longitudinally extended N1-surface which is parallel to the hydrophobic polyene chains (Fig. 4a). On the other hand, p-alagin is also characterized by an extended N1-surface surrounding the glucosidic moiety—hence the structure portion comprising the glucose unit and ester groups (Fig. 4b). The particular orientation of p-alagin carbonyl groups is also worth noting, and contributes to further increase the N1 interaction field (Fig. 4b right). In spite of the presence of 17 hydroxyl and 6 carbonyl groups conferring a substantially hydrophilic character to the p-alagin molecule, a hydrophobic region was detected around the ellagic moiety (Fig. 4b).

Thus, our calculations indicated that p-alagin and AmB are both amphiphilic and, more importantly, present a similar spatial arrangement of N1 and DRY molecular fields. The polar N1 field is longitudinally extended and almost parallel to the hydrophobic region, and is presumably responsible for similar aggregation properties. Analogously to the AmB aggregates reported by Baginski et al. (2002), p-alagin units may form pore-like structures in which the inner wall is formed by the glucoside unit, and the outer wall formed by the lasting moieties including the ellagic unit. The structure of a putative aggregate formed by eight units of p-alagin was also assembled by using molecular graphics tools (Fig. 5).

Conclusion

In vitro tests showed the ability of PAE to control *B. cinerea*. The effectiveness was also established by the treatment on fruits to extend the shelf life of strawberries. Furthermore, a high correlation between FT-NIR spectra and disease severity of fruits was shown, and provided a chemometric NIR model to predict disease severity on the fruit surface. In the future, more robust predictive models (with high variance percentage R squared) will be obtained by the employment of a wide range of standards. The identification of punicalagin as the prevalent component made it possible to propose hypotheses to explain the detected antifungal activity of pomegranate extract. By means of computational chemistry approaches, we showed that punicalagin and AmB are characterized by similar

Fig. 4 Molecular interaction fields calculated by using N1 (blue), O (yellow), and DRY (red) probes on the most representative structure of AmB (**a**) and p-alagin (**b**). MIFs are reported as isosurfaces (mesh)—isovalue of -3 , -3 , and -0.3 for the N1, O, and DRY field, respectively. 2D sketches of AmB and p-alagin displaying the regions with hydrophilic or hydrophobic character are also reported (color figure online)

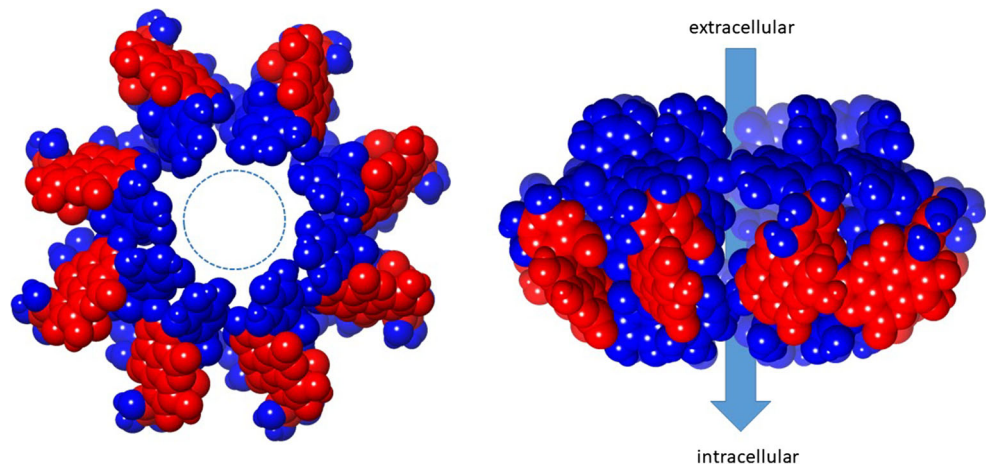


molecular interaction properties, probably connected to their ability to form pore-like aggregates.

The results obtained promote the use of natural extracts analyzed like fungicides to control postharvest fruits decay. Furthermore, to extend the shelf life of strawberry, we used

the extract with concentrations very similar to those recommended for chemicals. The substitution of synthetic pesticides with natural plant molecules significantly reduces the amount of chemicals in the environment and undesired effects such as the contamination of the food chain. Our

Fig. 5 Top (left) and side (right) view of a putative extramembrane aggregate formed by eight p-alagin units



study suggests that *P. granatum* peel extract could be an alternative to synthetic products to control postharvest deteriorations and improve postharvest quality of fruits by avoiding the impact of chemicals on human health. This is also an important target of the agricultural policies of the European Community.

Acknowledgments This work was supported by the projects “Difesa delle colture con prodotti naturali nella Regione Lazio (DI.CO.-PRO.NA.L) financed by the Lazio region.

References

- Anderson TM, Clay MC, Cioffi AG, Diaz KA, Hisao GS, Tuttle MD, Nieuwkoop AJ, Comellas G, Maryum N, Wang S, Uno BE, Wildeman EL, Gonen T, Rienstra CM, Burke MD (2014) Amphotericin forms an extramembranous and fungicidal sterol sponge. *Nat Chem Biol* 10(5):400–406
- Baginski M, Resat H, Borowski E (2002) Comparative molecular dynamics simulations of amphotericin B-cholesterol/ergosterol membrane channels. *Biochim Biophys Acta* 1567:63–78
- Bendini A, Cerretani L, Di Virgilio F, Belloni P, Bonoli-Carboognin M, Lercker G (2007) Preliminary evaluation of the application of the FT-IR Spectroscopy to control the geographic origin and quality of virgin olive oils. *J Food Qual* 30:424–437
- Berendsen HJC, Postma JPM, van Gunsteren WF, Di Nola A, Haak JR (1984) Molecular dynamics with coupling to an external bath. *J Chem Phys* 81:3684–3690
- Cross S, Cruciani G (2010) Molecular fields in drug discovery: getting old or reaching maturity? *Drug Discov Today* 15:23–32
- Darden TA, York DM, Pedersen LG (1993) Particle mesh Ewald: an Nlog(N) method for Ewald sums in large systems. *J Chem Phys* 98:10089–10092
- Daura X, Gademann K, Jaun B, Seebach D, van Gunsteren WF, Mark AE (1999) Peptide folding: when simulation meets experiment. *Angew Chem Int Ed* 38:236–240
- Di Qiu M, Shenkin P, Hollinger F, Still W (1997) Continuum model for solvation. A fast analytical method for the calculation of approximate Born radii. *J Phys Chem A* 101:3005–3014
- Fischer UA, Carle R, Kammerer DR (2011) Identification and quantification of phenolic compounds from pomegranate (*Punica granatum* L.) peel, mesocarp, aril and differently produced juices by HPLC-DAD-ESI/MSn. *Food Chem* 127:807–821
- Foss SR, Nakamura CV, Ueda-Nakamura T, Cortez DA, Endo EH, Dias Filho BP (2014) Antifungal activity of pomegranate peel extract and isolated compound punicalagin against dermatophytes. *Ann Clin Microbiol Antimicrob* 5:13–32
- Ghannoum MA, Rice LB (1999) Antifungal agents: mode of action, mechanisms of resistance, and correlation of these mechanisms with bacterial resistance. *Clin Microbiol Rev* 12(4):501–517
- Hartel S, Bolard J (1996) Amphotericin B: new life for an old drug. *Trends Pharmacol Sci* 17:445–449
- Helbig J (2002) Ability of the antagonistic yeast *Cryptococcus albidus* to control *Botrytis cinerea* in strawberry. *Biocontrol* 47:85–99
- Hess B, Bekker H, Berendsen HJC, Fraije JCEM (1997) LINCS: a linear constraint solver for molecular simulations. *J Comput Chem* 18:1463–1472
- Johnson L (2003) Dermatophytes—the skin eaters. *Mycologist* 17:147–149
- Jones E, Oliphant T, Peterson P (2001) SciPy: open source scientific tools for Python. <http://www.scipy.org/>
- Kaminski GA, Friesner RA, Tirado-Rives J, Jorgensen WL (2001) Evaluation and reparameterization of the OPLS-AA force field for proteins via comparison with accurate quantum chemical calculations on peptides. *J Phys Chem B* 105:6474–6487
- Landi L, Feliziani E, Romanazzi G (2014) Expression of defense genes in strawberry fruits treated with different resistance inducers. *J Agric Food Chem* 62:3047–3056
- Lopez-Reyes JG, Spadaro D, Gullino ML, Garibaldi A (2010) Efficacy of plant essential oils on postharvest control of rot caused by fungi on four cultivars of apples in vivo. *Flavour Fragr J* 25:171–177
- Marrone A, Re N, Storchi L (2016) The effects of Ca²⁺ concentration and E200K mutation on the aggregation propensity of PrPC: a computational study. *PLoS ONE* 11(12):e0168039. <https://doi.org/10.1371/journal.pone.0168039>
- Mlikota Gablera F, Smilanick JL, Mansourb MF, Karaca H (2010) Influence of fumigation with high concentrations of ozone gas on postharvest gray mold and fungicide residues on table grapes. *Postharvest Biol Technol* 55(2):85–90
- Nabigol A, Morshedi H (2011) Evaluation of the antifungal activity of the Iranian thyme essential oils on the postharvest pathogens of strawberry fruits. *Afr J Biotechnol* 10(48):9864–9869
- O’Boyle NM, Morley C, Hutchison GR (2008) Pybel: a Python wrapper for the OpenBabel cheminformatics toolkit. *Chem Cent J* 2:5–10
- Romanazzi G, Lichter A, Mlikota Gabler F, Smilanick JL (2012) Recent advances on the use of natural and safe alternatives to

- conventional methods to control postharvest gray mold of table grapes. *Postharvest Biol Technol* 63:141–147
- Romanazzi G, Feliziani E, Santini M, Landi L (2013) Effectiveness of postharvest treatment with chitosan and other resistance inducers in the control of storage decay of strawberry. *Postharvest Biol Technol* 75:24–27
- Romanazzi G, Smilanick JL, Feliziani E, Droby S (2016) Integrated management of postharvest gray mold on fruits crops. *Postharvest Biol Technol* 113:69–76
- Rongai D, Pulcini P, Pesce B, Milano F (2015) Antifungal activity of some botanical extracts on *Fusarium oxysporum*. *Open Life Sci (previously Cent Eur J Biol)* 10:409–416
- Rongai D, Pulcini P, Pesce B, Milano F (2017) Antifungal activity of pomegranate peel extract against fusarium wilt of tomato. *Eur J Plant Pathol* 147:229–238
- Storchi L, Paciotti R, Re N, Marrone A (2015) Investigation of the molecular similarity in closely related protein systems: the PrP case study. *Prot Struct Funct Bioinform* 83:1751–1765
- Van Der Spoel D, Lindahl E, Hess B, Groenhof G, Mark AE, Berendsen HJ (2005) GROMACS: fast, flexible, and free. *J Comput Chem* 26:1701–1718